

Robust Control of Rigid-Link Flexible-Joint Robots with Redundant Joint Actuators

Michael M. Bridges, Darren M. Dawson, Zhihua Qu, and Scott C. Martindale

Abstract—In this paper, we present an approach for designing robust tracking controllers for rigid-link flexible-joint (RLFJ) robot manipulators with redundant actuators in the joints. With the proposed controller, we prove that the link tracking error is globally uniformly ultimately bounded (GUUB) in spite of additive bounded disturbances, parametric uncertainty, and other modeling uncertainty. We also illustrate how the load at each joint is shared by two actuators. Finally simulation results are presented to illustrate the effectiveness of the proposed controller.

I. INTRODUCTION

IN recent years control engineers have become increasingly interested in the robot tracking problem. As a result many robot controllers have been developed which compensate for uncertainty in the nonlinear second order dynamics commonly used to represent rigid-link (RL) robots. Most of the more rigorously developed nonlinear controllers for RL robots fall into two categories, adaptive control and robust control. The interested reader is referred to [1] and [2] for review papers in these two areas.

In addition to developing controllers that can achieve good position tracking, researchers have also been interested in designing manipulators that can handle greater payloads. The use of gearing is a well established means for accomplishing such an objective; however, one of the biggest disadvantages in the use of standard gearing is the phenomena of “backlash.” Harmonic drives are a special type of gearing that have been shown to be virtually “backlash” free while still providing high gear ratios. A disadvantage of harmonic drives is that compliance or mechanical flexibility is introduced. A less common method for a further increase in the manipulator payload capacity is the use of the redundant actuators in the joints. This method effectively increases the maximum payload by distributing the weight between each actuator. However, two actuators coupled directly to one robot link further complicates the control problem by introducing additional actuator dynamics. Therefore, a control is required that can constructively generate torques for both actuators while ensuring good tracking. In general there is no particular weight savings gained by using two smaller motors instead

of a single larger motor, however the main benefit lies in the protection against total manipulator failure. That is, if one actuator should fail, the redundant actuator can be utilized to provide the required torque to maintain manipulator operation. Such reliability is often required in robotic space applications and a discussion of a manipulator equipped with redundant joint actuators can be found in [29]. This report details the efforts at Kennedy Space Center, where the robotics group has designed and constructed an Automated Radiator Inspection Device (ARID), to inspect radiator panels on the orbiter. Another potential benefit that has yet to be investigated is the possible cancellation of gyroscopic terms that are introduced by the spinning actuators. When formulating the robot/actuator model most commonly used in the literature, Spong, in [11], introduced a model simplification by neglecting the actuator gyroscopic terms. It is conceivable that with the introduction of an additional actuator, the mechanical configuration of the harmonic drive gearing can be arranged so that each actuator spins in opposite directions but applies positive torque to the link. The actuators gyroscopic terms would cancel each other out thereby making Spong’s simplified model even more valid. Since this paper is dealing mainly with controller design, we will address the manipulator design issues in future work.

Early work regarding the compensation of joint flexibilities can be found in [19]–[23]. Some recent work is now summarized. In [5], Readman shows that there exists a decentralized velocity control law for RLFJ robots which asymptotically stabilizes the flexible joint dynamics if the actuator drive inertia matrix is sufficiently small. In [6], Mrad designs an adaptive controller for RLFJ robots; however, the proposed control law is not well defined. Furthermore, since the control law contains variable structure-like terms, the control input will exhibit an undesirable chattering phenomenon. A comprehensive study of adaptive control of RLFJ robots is given in [30]. In [7], Ghorbel and Spong show asymptotic link tracking can be achieved by modifying an RL adaptation law and by assuming the desired link trajectory approaches zero as time approaches infinity. In [17], Benallegue and M’Sirdi design a GAS adaptive controller based on the passivity approach; however, this approach requires measurement of link acceleration and link jerk. In [18], Chen and Fu use an approach similar to the one given in this paper; however, the stability result is local, and the controller requires measurement of acceleration. In [3], Dawson, *et al.* design a hybrid adaptive RLFJ controller that achieves GAS position tracking. The controller is hybrid in the sense that an adaptive technique is used to compensate for parametric uncertainty in the robot

Manuscript received March 13, 1992; revised August 16, 1993. This work was supported in part by the National Science Foundation under Grants MSS-9110034 and IRI-9111258, and by the U.S. Department of Education under a Patricia Roberts Harris Fellowship.

M. M. Bridges, D. M. Dawson, and S. C. Martindale are with the School of Electrical and Computer Engineering, Clemson University, Clemson, SC 29634 USA.

Z. Qu is with the Department of Electrical Engineering, University of Central Florida, Orlando, FL 32816 USA.

IEEE Log Number 9401965.

model while a robust technique is used to compensate for the actuator dynamics. In [4], Dawson *et al.* design a robust RLFJ controller that compensates for parametric uncertainty, model uncertainty and unknown bounded disturbances in both the manipulator and actuator dynamics. In [28], Lozano designed an adaptive controller for n -link RLFJ robots.

It should be noted that recently, in several theoretical control papers [24]–[27], researchers have designed new control techniques for systems that meet the so-called extended matching conditions. In fact, one can easily establish that the RLFJ controllers in [3], [4], [17], [18], and [28] are directly related to these new control techniques. This paper extends the results obtained in [4] to a RLFJ manipulator with redundant joint actuators. That is, we design a robust tracking controller for two actuators driving the same joint. We then show that the link tracking error is GUUB stable in spite of parametric uncertainties and additive bounded disturbances. The paper is organized as follows. In Section II, we describe the robot and actuator models and give some mathematical preliminaries. In Section III, we design a robust tracking controller for each actuator that compensates for uncertainty present in the RLFJ model and present the stability analysis. In Section IV, we discuss load sharing ramifications. Finally in Section V, we present simulation results to validate the effectiveness of the proposed controller.

II. MATHEMATICAL PRELIMINARIES

In this section, we give the model for RLFJ robots with redundant actuators in each joint. We also present some physical properties that will be exploited in the subsequent robust control synthesis. The model for the RLFJ robot given in [11], modified to include an additional motor and gearing (see Fig. 1), is given by

$$\begin{aligned} M(q)\ddot{q} + V_m(q, \dot{q})\dot{q} + G(q) + F(\dot{q}) + T_L \\ = K_1(\Gamma_1 q_{m1} - q) + K_2(\Gamma_2 q_{m2} - q), \end{aligned} \quad (2.1)$$

$$J_1 \ddot{q}_{m1} + B_1 \dot{q}_{m1} + \Gamma_1 K_1(\Gamma_1 q_{m1} - q) + T_{m1} = u_{m1}, \quad (2.2)$$

and

$$J_2 \ddot{q}_{m2} + B_2 \dot{q}_{m2} + \Gamma_2 K_2(\Gamma_2 q_{m2} - q) + T_{m2} = u_{m2}. \quad (2.3)$$

$M(q)$ is an $n \times n$ link inertia matrix, $V_m(q, \dot{q})$ is an $n \times n$ matrix containing the centripetal and Coriolis terms, $G(q)$ is an $n \times 1$ vector containing the gravity terms, $F(\dot{q})$ is an $n \times 1$ vector containing the static and dynamic friction terms, T_L is an unknown bounded disturbance torque at the link level, and $q(t)$ is an $n \times 1$ vector representing the link displacements. Given the addition of an extra actuator to each joint, we now introduce the subscript i to differentiate between actuator parameters. Let $i = 1$ represent the primary actuator in each joint and $i = 2$ the secondary actuator. We can now define K_i as an $n \times n$ positive-definite constant diagonal matrix used to denote the joint flexibilities in each actuator, and Γ_i to be an $n \times n$ positive-definite constant diagonal matrix used to represent the gear ratio in each actuator. Similarly, $q_{mi}(t)$ is an $n \times 1$ vector representing the actuator displacements, J_i is an $n \times n$ positive-definite constant diagonal actuator inertia

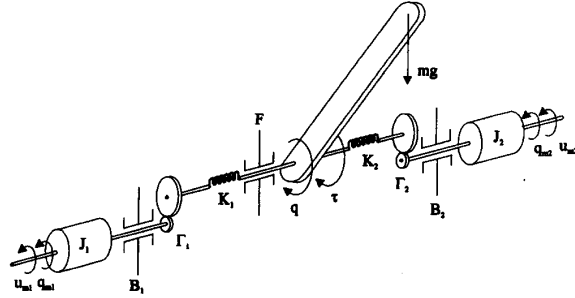


Fig. 1. Model of a redundant flexible joint robot.

matrix, B_i is a positive-definite constant diagonal $n \times n$ matrix used to represent the actuator damping, T_{mi} is an unknown bounded disturbance torque at the actuator, and $u_{mi}(t)$ is an $n \times 1$ control vector used to represent the torque provided by the primary and secondary actuators in each joint.

For the remainder of this paper, we will find it convenient to represent the manipulator dynamics of (2.1) as

$$\begin{aligned} M(q)\ddot{q} + V_m(q, \dot{q})\dot{q} + G(q) + F(\dot{q}) + T_L \\ = \bar{K}_1(q_{m1} - \Gamma_1^{-1}q) + \bar{K}_2(q_{m2} - \Gamma_2^{-1}q) \end{aligned} \quad (2.4)$$

where $\bar{K}_i = K_i \Gamma_i$ represents a modified diagonal positive definite flexibility matrix.

The robotic controls literature [8] has placed much emphasis on the use of physical properties of the robot manipulator to aid in stability analysis. Therefore, we now note some of these properties.

Property 1—Inertia

The inertia matrix $M(q)$, defined in (2.1), is symmetric, positive definite, and uniformly bounded by a function of q , i.e.,

$$\begin{aligned} m_L \|x\|^2 &= \lambda \min \{M(q)\} \|x\|^2 \leq x^T M(q) x \\ &\leq \lambda \max \{M(q)\} \|x\|^2 = m_U(q) \|x\|^2; \end{aligned} \quad (2.5)$$

where m_L is a positive scalar constant, $m_U(q)$ is a positive scalar function that depends on the mass properties of the specific robot, x is an arbitrary $n \times 1$ vector, and $\|\cdot\|$ is used to denote the Euclidean norm [16].

Property 2—Skew Symmetric

A useful relationship exists between the time derivative of the inertia matrix $M(q)$ and the Coriolis/centripetal matrix $V_m(q, \dot{q})$. The following quadratic form is equal to zero:

$$x^T (\dot{M}(q) - 2V_m(q, \dot{q})) x = 0 \quad (2.6)$$

for an arbitrary $n \times 1$ vector x .

It is important to emphasize that in many real world problems, one cannot always exactly determine the parameters in an assumed model. In spite of this uncertainty, it is assumed that bounds do exist for each of these “uncertain” quantities. For example, the modified joint flexibility matrix, defined in

(2.4) for each set of actuators, is assumed to be bounded as shown

$$\begin{aligned} \bar{k}_{Li} \|x\|^2 &= \lambda \min \{\bar{K}_i\} \|x\|^2 \leq x^T \bar{K}_i x \\ &\leq \lambda \max \{\bar{K}_i\} \|x\|^2 = \bar{k}_{Ui} \|x\|^2; \end{aligned} \quad (2.7)$$

where \bar{k}_{Li} and \bar{k}_{Ui} are positive scalar bounding constants that depend on the flexibility constants and gear ratios associated with each actuator. It will also be useful to define a composite matrix as

$$\bar{K}_T = \bar{K}_1 + \bar{K}_2 \quad (2.8)$$

where

$$\begin{aligned} \bar{k}_{TL} \|x\|^2 &= \lambda \min \{\bar{K}_T\} \|x\|^2 \leq x^T \bar{K}_T x \\ &\leq \lambda \max \{\bar{K}_T\} \|x\|^2 = \bar{k}_{TU} \|x\|^2, \end{aligned} \quad (2.9)$$

and

$$\bar{k}_{TL} = \bar{k}_{L1} + \bar{k}_{L2} \quad \text{and} \quad \bar{k}_{TU} = \bar{k}_{U1} + \bar{k}_{U2}. \quad (2.10)$$

The actuator inertia matrix J_i in (2.2) and (2.3) can also be bounded by

$$\begin{aligned} j_{Li} \|x\|^2 &= \lambda \min \{J_i\} \|x\|^2 \leq x^T J_i x \\ &\leq \lambda \max \{J_i\} \|x\|^2 = j_{Ui} \|x\|^2 \end{aligned} \quad (2.11)$$

where j_{Li} and j_{Ui} are positive scalar bounding constants. The parametric bounds given by (2.5), (2.7), (2.9), and (2.11) will be exploited later in the controller development.

III. ROBUST CONTROL DEVELOPMENT AND STABILITY ANALYSIS

In this section, we design a corrective robust tracking controller for the actuators in each joint to compensate for uncertainties in the RLFJ robot model. The proposed controller is robust with regard to parametric uncertainties and additive bounded disturbances while correcting for joint flexibilities. That is, in spite of these model uncertainties and additional actuator dynamics, we show that the link tracking error has a GUUB stability property. We then illustrate the usefulness of this stability property by showing how the controller gains can be adjusted to improve tracking performance.

A. Controller Development

We now formulate the error system that will be used in the stability analysis, keeping in mind that our control objective is to maintain good link position tracking in spite of parametric uncertainties, additive bounded disturbances, and joint flexibilities. We start the controller development by defining the link position tracking error to be

$$e_L = q_d - q \quad (3.1)$$

where q_d is an $n \times 1$ vector used to represent the desired link position trajectory. We will assume that q_d and its first, second, and third derivatives are all bounded functions of time. This assumption on the ‘‘smoothness’’ of the desired trajectory ensures that the controller, to be defined later,

remains bounded. We begin the error system formulation by defining an $n \times 1$ filtered tracking error vector [8] as

$$r_L = \alpha e_L + \dot{e}_L \quad (3.2)$$

where α is a positive scalar constant. We can now rewrite (2.4) in terms of (3.2) to yield

$$M(q)\dot{r}_L = -V_m(q, \dot{q})r_L + w_L - \bar{K}_1 z_1 - \bar{K}_2 z_2, \quad (3.3)$$

where

$$\begin{aligned} w_L &= M(q)(\ddot{q}_d + \alpha \dot{e}_L) + V_m(q, \dot{q})(\dot{q}_d + \alpha e_L) \\ &\quad + G(q) + F(\dot{q}) + T_L, \end{aligned} \quad (3.4)$$

$$z_1 = q_{m1} - \Gamma_1^{-1} q, \quad \text{and} \quad z_2 = q_{m2} - \Gamma_2^{-1} q. \quad (3.5)$$

One can see that there is no control input in (3.3); therefore we will add and subtract the terms $1/2\bar{K}_i u_L$ on the right-hand side of (3.3) for $i = 1, 2$ to yield

$$\begin{aligned} M(q)\dot{r}_L &= -V_m(q, \dot{q})r_L + w_L - \frac{1}{2}\bar{K}_1 u_L \\ &\quad + \bar{K}_1 \left(\frac{1}{2}u_L - z_1\right) - \frac{1}{2}\bar{K}_2 u_L \\ &\quad + \bar{K}_2 \left(\frac{1}{2}u_L - z_2\right) \end{aligned} \quad (3.6)$$

where the embedded control input u_L is an $n \times 1$ vector to be defined later. This embedded input can be viewed as a robust controller that specifies a link torque. If this control torque could be applied directly to the links, it would provide good link tracking in spite of model uncertainty and additive bounded disturbances. Given that the only way to supply a torque to the link of the robot is through the two actuators, we formulate a strategy that forces each actuator to provide approximately half of the desired control torque. As we will see later, this controller u_L is actually embedded inside the overall control strategy which is designed at u_{m1} and u_{m2} , the torque input level for both joint actuators.

From (3.6), we can see that if we define two perturbation terms as

$$\eta_i = \frac{1}{2}u_L - z_i \quad \text{for } i = 1, 2 \quad (3.7)$$

then our goal is to force η_i to become ‘‘small’’ (i.e., GUUB). One can see from (3.6) that when this is accomplished, each actuator is providing approximately its share of the desired control torque. This control torque will be specified by a previously defined robust control algorithm [13] that has been shown to ensure GUUB link tracking.

To force η_i to be GUUB, the dynamics of the perturbation terms are needed; therefore, we differentiate (3.7) to yield

$$\dot{\eta}_i = \frac{1}{2}\dot{u}_L - \dot{z}_i. \quad (3.8)$$

As before we can add and subtract an $n \times 1$ vector w_{η_i} to the right-hand side of (3.8). In addition, we add and subtract $\bar{K}_i r_L$ to eliminate cross terms that appear later in the stability analysis to yield

$$\dot{\eta}_i = w_{\eta_i} - \bar{K}_i r_L - u_{\eta_i} + (u_{\eta_i} - \dot{z}_i) \quad (3.9)$$

where

$$w_{\eta_i} = \frac{1}{2}\dot{u}_L + \bar{K}_i r_L. \quad (3.10)$$

The $n \times 1$ vector u_{η_i} is defined to be another embedded robust controller of the same form as u_L , but designed to make η_i GUUB. An examination of (3.9) reveals a second perturbation term ($u_{\eta_i} - \dot{z}_i$) which also needs to be controlled. This perturbation term is defined as follows:

$$\Pi_i = u_{\eta_i} - \dot{z}_i. \quad (3.11)$$

If we proceed as previously outlined, (3.11) is differentiated to obtain

$$\dot{\Pi}_i = \dot{u}_{\eta_i} - \ddot{z}_i. \quad (3.12)$$

We can now substitute the actuator dynamics of (2.2) and (2.3) into (3.12). In addition, we can utilize (2.1) and (3.5), multiply both sides by J_i , and add and subtract η_i to the right-hand side for cross term elimination to yield

$$J_i \dot{\Pi}_i = w_{\pi_i} - \eta_i - u_{m_i} \quad (3.13)$$

where

$$\begin{aligned} w_{\pi_i} = & J_i \dot{u}_{\eta_i} + B_i \dot{q}_{m_i} + \Gamma_i K_i (\Gamma_i q_{m_i} - q) \\ & + T_{m_i} + \eta_i + J_i \Gamma_i^{-1} M^{-1}(q) \\ & \cdot [\bar{K}_1 z_1 + \bar{K}_2 z_2 - V_m(q, \dot{q}) \dot{q} - G(q) \\ & - F(\dot{q}) - T_L]. \end{aligned} \quad (3.14)$$

The $n \times 1$ vector u_{m_i} is the final robust controller applied to each actuator at the torque input level. This controller is designed to force Π_i to become GUUB.

Now that we have formulated the error system [i.e., (3.6), (3.9), and (3.13)], we define the robust controllers for $i = 1, 2$ to be

$$\begin{aligned} u_L &= \bar{k}_{TL}^{-1} [k_L \gamma_2(\|x\|) r_L + v_L], \\ u_{\eta_i} &= k_{\eta_i} \gamma_2(\|x\|) \eta_i + v_{\eta_i}, \end{aligned}$$

and

$$u_{m_i} = k_{\pi_i} \gamma_2(\|x\|) \Pi_i + v_{\pi_i}, \quad (3.15)$$

where k_L , k_{η_i} , and k_{π_i} are positive gain constants, $x = [r_L^T, \eta_1^T, \eta_2^T, \Pi_1^T, \Pi_2^T]^T$, and $\gamma_2(\|x\|)$ is a strictly positive scalar function defined as follows:

$$\gamma_2(\|x\|) \geq \frac{1}{2} \max \{m_2(q), 1, j_{U1}, j_{U2}\}. \quad (3.16)$$

The auxiliary control terms v_L , v_{η_i} , and v_{π_i} defined in (3.15) are used to compensate for parametric uncertainty, additive disturbances, and actuator dynamics. These auxiliary controllers are defined as [12]

$$\begin{aligned} v_L &= \frac{2r_L \rho_L^2}{\rho_L \|r_L\| + \epsilon_L}, \\ v_{\eta_i} &= \frac{\eta_i \rho_{\eta_i}^2}{\|\eta_i\| \rho_{\eta_i} + \epsilon_{\eta_i}}, \end{aligned}$$

and

$$v_{\pi_i} = \frac{\Pi_i \rho_{\pi_i}^2}{\|\Pi_i\| \rho_{\pi_i} + \epsilon_{\pi_i}}, \quad (3.17)$$

where ϵ_L , ϵ_{η_i} , and ϵ_{π_i} are positive scalars which are adjusted to achieve a desired tracking performance. The positive scalar

functions ρ_L , ρ_{η_i} and ρ_{π_i} are used to "bound" the uncertainty in the RLFJ model. These bounding functions are defined as

$$\rho_L \geq \|w_L\|, \quad \rho_{\eta_i} \geq \|w_{\eta_i}\|, \quad \text{and} \quad \rho_{\pi_i} \geq \|w_{\pi_i}\| \quad (3.18)$$

where w_L , w_{η_i} , and w_{π_i} are defined in (3.4), (3.10), and (3.14).

Remark 3.1: Later in this section, we will discuss how to calculate the bounding functions in (3.18). For now, we simply assume their existence. It should be emphasized that the bounding functions depend only on measurements of q_{m_i} , \dot{q}_{m_i} , q , and \dot{q} . At first, it may appear that the bounding functions ρ_{η_i} and ρ_{π_i} require measurement of link acceleration and jerk because of the terms \dot{u}_L , and \dot{u}_{η_i} given in (3.10) and (3.14). However, we will show later that we only require an upper bound on these terms which can be written entirely in terms of q_{m_i} , \dot{q}_{m_i} , q , and \dot{q} .

B. Stability Analysis

We now show that the robust controllers given in (3.15) have a GUUB [12] property for the tracking error systems given by (3.6), (3.9), and (3.13). It should be emphasized that the robust controllers do not require exact knowledge for any of the dynamics described by (2.1), (2.2), and (2.3). Due to the fact that w_L , w_{η_i} , and w_{π_i} in (3.4), (3.10), and (3.14) contain unknown parameters and disturbances, there may be some "uncertainty" associated with these terms. However, using the bounds on the uncertainty given in (3.16) and (3.18), the robust controllers given in (3.15) still ensure good tracking performance.

Using Lyapunov stability analysis, we now show that the link position tracking error defined by (3.1) is GUUB.

Theorem 3.1: The state vector $x = [r_L^T, \eta_1^T, \eta_2^T, \Pi_1^T, \Pi_2^T]^T$ is GUUB in the sense of Lemma A.1 in Appendix A with

$$\lambda_1 = \frac{1}{2} \min \{m_1, 1, j_{L1}, j_{L2}\}, \quad (3.19)$$

$$\gamma_2(\|x\|) \geq \frac{1}{2} \max \{m_2(q), 1, j_{U1}, j_{U2}\}, \quad (3.20)$$

$$\lambda_3 = \min \left\{ \frac{1}{2} k_L, k_{\eta_1}, k_{\eta_2}, k_{\pi_1}, k_{\pi_2} \right\}, \quad (3.21)$$

and

$$\epsilon = \epsilon_L + \epsilon_{\eta_1} + \epsilon_{\eta_2} + \epsilon_{\pi_1} + \epsilon_{\pi_2}. \quad (3.22)$$

Proof: Select the Lyapunov function candidate

$$V = x^T P x \quad (3.23)$$

where the $5n \times 5n$ matrix P is given by

$$P = \frac{1}{2} \text{block diag} \{M(q), I_{n \times n}, I_{n \times n}, J_1, J_2\}, \quad (3.24)$$

and $I_{n \times n}$ is the $n \times n$ identity matrix. The Lyapunov function given in (3.23) can be bounded as

$$\lambda_1 \|x\|^2 \leq V(x(t), t) \leq \gamma_2(\|x\|) \|x\|^2 \quad (3.25)$$

where λ_1 and $\gamma_2(\|x\|)$ are given in (3.19) and (3.20). Differentiating (3.23) with respect to time yields

$$\begin{aligned} \dot{V} = & \frac{1}{2} r_L^T \dot{M}(q) r_L + r_L^T M(q) \dot{r}_L \\ & + \sum_{i=1}^2 [\eta_i^T \dot{\eta}_i + \Pi_i^T J_i \dot{\Pi}_i]. \end{aligned} \quad (3.26)$$

Substituting (3.6), (3.9), (3.13), and (3.15) into (3.26) and using Property 2 yields

$$\begin{aligned} \dot{V} = & \sum_{i=1}^2 \left[-\frac{1}{2} r_L^T \bar{K}_i \bar{k}_{TL}^{-1} (k_L \gamma_2 (\|x\|) r_L + v_L) \right. \\ & \left. - \eta_i^T k_{\eta i} \gamma_2 (\|x\|) \eta_i - \Pi_i^T k_{\pi i} \gamma_2 (\|x\|) \Pi_i \right] tr_L^T w_L \\ & + \sum_{i=1}^2 \left[r_L^T \bar{K}_i \eta_i + \eta_i^T w_{\eta i} - \eta_i^T v_{\eta i} - \eta_i^T \bar{K}_i r_L \right. \\ & \left. + \eta_i^T \Pi_i + \Pi_i^T w_{\pi i} - \Pi_i^T v_{\pi i} - \Pi_i^T \eta_i \right]. \end{aligned} \quad (3.27)$$

We can now give an expression for the upper bound on \dot{V} as

$$\begin{aligned} \dot{V} \leq & -\gamma_2 (\|x\|) \sum_{i=1}^2 \left[\frac{1}{2} \lambda_{\min} \{ \bar{K}_i \} \bar{k}_{TL}^{-1} k_L \|r_L\|^2 \right. \\ & \left. + k_{\eta i} \|\eta_i\|^2 + k_{\pi i} \|\Pi_i\|^2 \right] \\ & + \|r_L\| \|w_L\| + \sum_{i=1}^2 \left[-\frac{1}{2} r_L^T \bar{K}_i \bar{k}_{TL}^{-1} v_L + \|\eta_i\| \|w_{\eta i}\| \right. \\ & \left. - \eta_i^T v_{\eta i} + \|\Pi_i\| \|w_{\pi i}\| - \Pi_i^T v_{\pi i} \right]. \end{aligned} \quad (3.28)$$

Lemma B.1 from Appendix B illustrates that the third and fourth line of (3.28) can be upper bounded as

$$\begin{aligned} \|r_L\| \|w_L\| + \sum_{i=1}^2 \left[-\frac{1}{2} r_L^T \bar{K}_i \bar{k}_{TL}^{-1} v_L + \|\eta_i\| \|w_{\eta i}\| \right. \\ \left. - \eta_i^T v_{\eta i} + \|\Pi_i\| \|w_{\pi i}\| - \Pi_i^T v_{\pi i} \right] < \epsilon, \end{aligned} \quad (3.29)$$

where ϵ is defined in (3.22). From (2.8), (2.9), (2.10), (3.28) and (3.29), we can establish the following upper bound on \dot{V} :

$$\dot{V} \leq \gamma_2 (\|x\|) x_n^T Q x_n + \epsilon \quad (3.30)$$

where 5×5 matrix Q is defined by

$$Q = \text{diag} \left\{ \frac{1}{2} k_L, k_{\eta 1}, k_{\eta 2}, k_{\pi 1}, k_{\pi 2} \right\}, \quad (3.31)$$

and

$$x_n = [\|r_L\|, \|\eta_1\|, \|\eta_2\|, \|\Pi_1\|, \|\Pi_2\|]^T. \quad (3.32)$$

Since all of the controller gains are positive, the matrix Q defined in (3.31) is positive definite; consequently, it can also be shown that

$$-x_n^T Q x_n \leq -\lambda \min \{Q\} \|x_n\|^2 \quad \text{and} \quad \|x_n\|^2 = \|x\|^2. \quad (3.33)$$

Using (3.33), we can obtain a new upper bound on \dot{V} written as

$$\dot{V} \leq \lambda_3 \gamma_2 (\|x\|) \|x\|^2 + \epsilon \quad (3.34)$$

where $\lambda_3 = \lambda \min \{Q\}$ is defined in (3.21). Applying Lemma A.1 to (3.25) and (3.34) yields Theorem 3.1.

Remark 3.2: Theorem 3.1 not only allows us to show that x is GUUB but also allows us to comment on its transient response. Specifically, Lemma A.1 gives an expression that shows how $\|x\|$ is bounded by an exponentially decaying envelope which forces it into a ball where it remains for all times thereafter. The rate at which this envelope decays is defined by λ_3 given in (3.21). An examination of (3.21) shows us that we can speed up the transient response by increasing the controller gains $k_L, k_{\eta 1}, k_{\eta 2}, k_{\pi 1}$, and $k_{\pi 2}$. It should also be noted that we can control the size of the ball in which $\|x\|$ ultimately remains. The size of this final ball is defined as

$$B_0 = \sqrt{\frac{\epsilon}{\lambda_1 \lambda_3}}. \quad (3.35)$$

As we can see from (3.35) and (3.21), increasing the controller gains also reduces the size of the error ball. Because we have control over ϵ which is defined in (3.22), we can also reduce the size of the error ball by making this parameter small. The only other parameter which has an effect on the size of the error ball is λ_1 which is determined by the robot and actuator model parameters.

Remark 3.3: The stability result given in Theorem 3.1 informs us that the vector $\|x\|$ is GUUB; and consequently, the filtered link tracking error $\|r_L\|$ is GUUB. However, we are really more concerned with the response of the position tracking error defined in (3.1). Note that from Lemma A.1, we can obtain an upper bound on $\|x\|$ and $\|r_L\|$ as

$$\|r_L(t)\| \leq \|x(t)\| \leq \sqrt{a} + \sqrt{b} \exp(-\lambda_3 t/2) \quad (3.36)$$

where

$$\begin{aligned} a &= \frac{\epsilon}{\lambda_1 \lambda_3}, \\ b &= \left| \frac{\gamma_2 (\|x(0)\|)}{\lambda_1} \|x(0)\|^2 - \frac{\epsilon}{\lambda_1 \lambda_3} \right|, \end{aligned} \quad (3.37)$$

$\lambda_1, \gamma_2 (\|x\|)$, and λ_3 are defined in (3.19), (3.20), and (3.21). Now it is easy to show by standard linear control arguments [16] and the definition of the filtered tracking error in (3.2) that

$$\begin{aligned} \|e_L(t)\| &\leq n \exp(-\alpha t) \|e_L(0)\| \\ &+ n \int_0^t \exp(-\alpha t + \alpha \sigma) \|r_L(\sigma)\| d\sigma \end{aligned} \quad (3.38)$$

where n is equal to the number of robot joints. Substituting (3.36) into (3.38), it is easy to show that

$$\begin{aligned} \|e_L(t)\| &\leq n \exp(-\alpha t) \|e_L(0)\| \\ &+ n \frac{\sqrt{a}}{\alpha} [1 - \exp(-\alpha t)] \\ &+ \frac{2n\sqrt{b}}{2\alpha - \lambda_3} [\exp(-\lambda_3 t/2) - \exp(-\alpha t)]. \end{aligned} \quad (3.39)$$

From (3.39), it can now be shown that increasing the controller gains $k_L, k_{\eta 1}, k_{\eta 2}, k_{\pi 1}, k_{\pi 2}, \alpha$ and decreasing ϵ , speed up the transient response of the position tracking error and also decrease the size of the ball that the position tracking error is ultimately confined in.

□

Remark 3.4: It should be noted that we can obtain an upper bound on the performance of the velocity tracking error (\dot{e}_L) by simply applying a triangle inequality type argument [16] to (3.2). Specifically, we can state that

$$\|\dot{e}_L(t)\| \leq \alpha \|e_L(t)\| + \|r_L(t)\|. \quad (3.40)$$

We can now use (3.36) and (3.39) to develop a GUUB stability argument for the velocity tracking error.

D. Formulation of Bounding Functions

We now illustrate how the bounding functions given in (3.18) can be found. With regard to $\rho_L \geq \|w_L\|$, it has been shown [13] that

$$\rho_L = \zeta_2 \|e_L\|^2 + \zeta_1 \|e_L\| + \zeta_0 \quad (3.41)$$

where ζ_2, ζ_1 , and ζ_0 are positive scalar constants that depend on estimates of the upper bounds on parametric quantities such as the largest payload mass.

We will not give a general expression for $\rho_{\eta_1}, \rho_{\eta_2}, \rho_{\pi_1}$, and ρ_{π_2} ; however, we will outline a procedure for finding this function. By using (2.4), it can easily be established that all of the dynamics in (3.10) and (3.14) can be bounded by combinations of constants and functions of the measurable quantities $q, \dot{q}, q_{m1}, q_{m2}, \dot{q}_{m1}$, and \dot{q}_{m2} . For example, we are required to bound w_{η_1} and w_{η_2} defined in (3.10). Since w_{η_i} contains the term $\frac{1}{2}\dot{u}_L$, the corresponding bounding function ρ_{η_i} defined in (3.18) would seem to be a function of link acceleration. However, since we only need an upper bound on acceleration, we can use (2.4) to obtain this upper bound. Specifically, by rewriting (2.4) and (3.5) into the form

$$\ddot{q} = M(q)^{-1}[\bar{K}_1 z_1 + \bar{K}_2 z_2 - V_m(q, \dot{q})q - G(q) - F(\dot{q}) - T_L]. \quad (3.42)$$

We can use the right-hand side of (3.42) to bound \ddot{q} by constants and functions of the measurable states. That is, we can define an upper bound on link acceleration as

$$\|\ddot{q}\| \leq f_a(q, \dot{q}, q_{m1}, q_{m2}). \quad (3.43)$$

As a result of (3.43), the bounding functions ρ_{η_1} and ρ_{η_2} do not depend on link acceleration. By utilizing (3.43), the bounding functions ρ_{π_1} and ρ_{π_2} defined in (3.18) can similarly be found to be only dependent on $q, \dot{q}, q_{m1}, q_{m2}, \dot{q}_{m1}$, and \dot{q}_{m2} .

Remark 3.5: The calculation of the robust controllers defined in (3.15) is slightly complicated by the fact that we must calculate bounds on the derivative of the embedded robust controllers (i.e., u_L, u_{η_i}). In general, the embedded controllers will be functions of the Euclidean norm of states; therefore, in general, the derivative of these terms are not well-defined. This problem can be eliminated by redefining v_L in (3.17) to

$$v_L = \frac{2r_L \rho_{L_s}^2}{\rho_{L_m} \|r_L\|_m + \epsilon_L} \quad (3.44)$$

where ρ_{L_s} and ρ_{L_m} are the same positive scalar function defined in (3.18) (i.e., ρ_L) but with the standard Euclidean norm being replaced by the norm functions $\|\cdot\|_s$ and $\|\cdot\|_m$,

respectively. The norm functions $\|\cdot\|_s$ and $\|\cdot\|_m$ are defined to be

$$\|y\|_s = \sqrt{y^T y + \sigma}$$

and

$$\|y\|_m = \sqrt{y^T y + \sigma} - \sqrt{\sigma} \quad (3.45)$$

where σ is a small positive constant, and y is an arbitrary $n \times 1$ vector. Note that as a result of (3.45) and the standard definition of the Euclidean norm, we have

$$\|y\|_s \geq \|y\| \geq \|y\|_m \quad (3.46)$$

and

$$\rho_{L_s} \geq \rho_L \geq \rho_{L_m}. \quad (3.47)$$

It should be noted that the redefining of v_L in no way destroys the stability result given by Theorem 3.1. This can be established by noting that

$$\frac{2\|r_L\|^2 \rho_{L_s}^2}{\rho_{L_m} \|r_L\|_m + \epsilon_L} \geq \frac{2\|r_L\|^2 \rho_L^2}{\rho_L \|r_L\| + \epsilon_L}. \quad (3.48)$$

That is, after retracing the steps of the proof of Theorem 3.1 with v_L given by (3.44), we can utilize (3.48) to replace the quantity on the left-hand side of (3.48) with the quantity on the right-hand side of (3.48) to yield a new upper bound on \dot{V} in (3.28). Hence, the rest of the proof of Theorem 3.1 then follows. The same type of modification given in (3.48) can be made to v_{η_i} defined in (3.17) to ensure that the derivative of u_{η_i} exists. Likewise, the scalar function $\gamma_2(\|x\|)$, defined in (3.16), is modified to be a function of $\|x\|_s$.

IV. LOAD SHARING RAMIFICATIONS

Given that two actuators are present in each joint and are of similar size, the torque that can be generated has effectively been doubled. An important concern is the distribution of load between each joint actuator. If we examine (3.5) and (3.7), it can be shown that the difference between the shaft torsional windup of each actuator can be upper bounded as

$$\|z_2 - z_1\| = \left\| \left(\frac{1}{2} u_L - z_1 \right) - \left(\frac{1}{2} u_L - z_2 \right) \right\| \leq \|\eta_1\| + \|\eta_2\|. \quad (4.1)$$

Because $\|\eta_1\|$ and $\|\eta_2\|$ are shown to be GUUB by Theorem 3.1, then the torsional difference $\|z_2 - z_1\|$ is also GUUB. Since the ball in which this difference is ultimately confined in is small, we can make the assumption that $z_1 \approx z_2$. Further examination of (2.1) shows that the torque supplied to the link by each actuator can be expressed as

$$\tau_1 = \bar{K}_1 z_1 \quad \text{and} \quad \tau_2 = \bar{K}_2 z_2 \quad (4.2)$$

where τ_1 and τ_2 are $n \times 1$ vectors that represent the torque supplied to each joint by the primary and secondary actuators, respectively. One can see from (4.2) that if $z_1 \approx z_2$ then the difference in torque supplied by the actuators is mainly due to the difference in actuator modified flexibility matrices \bar{K}_1 and \bar{K}_2 . Consequently, the primary and secondary actuators will

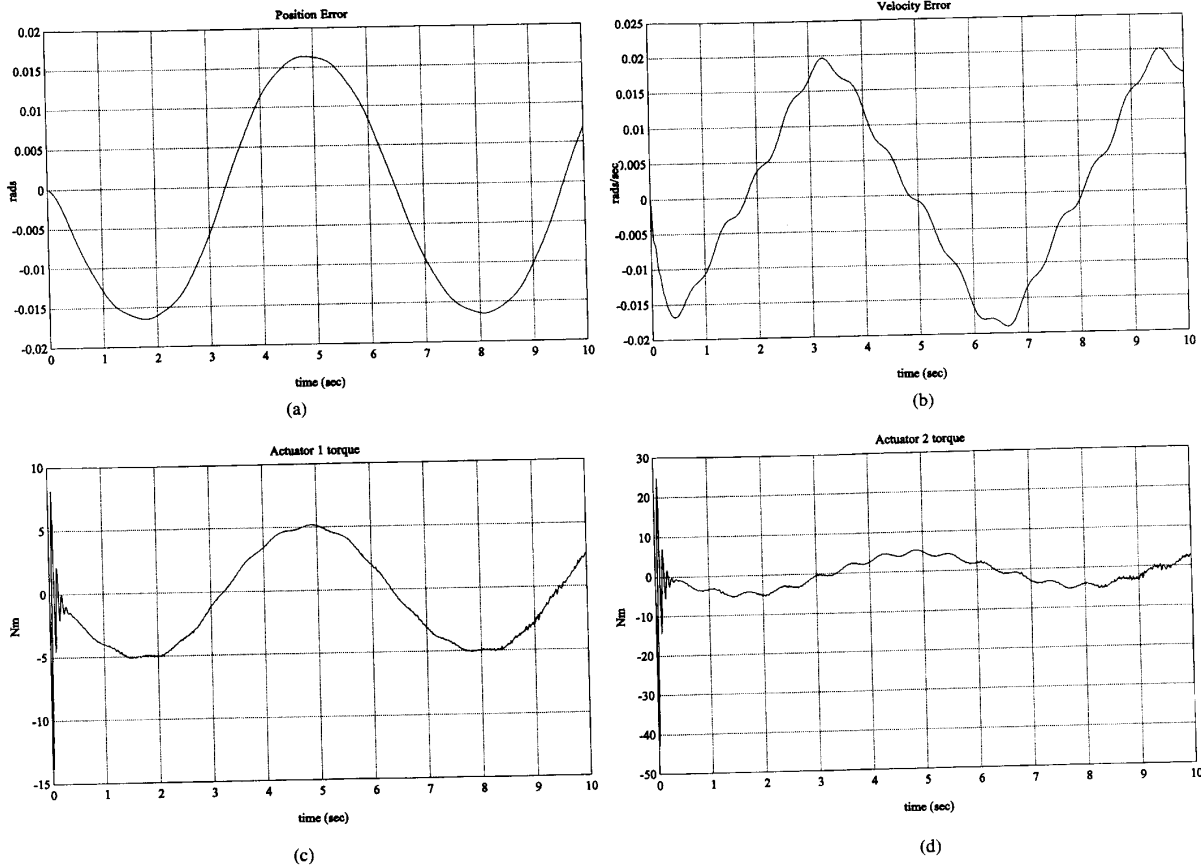


Fig. 2. Simulation results for both actuator 1 and actuator 2 operational.

more equally share the link load if their corresponding gear ratios and flexibility constants are similar.

V. SIMULATION

In this section, we give simulation results for the theoretical developments presented in Section II for a revolute, signal link flexible joint robot arm equipped with two actuators. It should be noted that we neglect friction in the simulation. The following parameters were used in the simulation:

$$\begin{aligned} \epsilon_L &= 0.01, \epsilon_{\eta_i} = 0.1, \epsilon_{\pi_i} = 0.1, \\ J_i &= 1.0 \text{ Kg-m}^2, M = 1.0 \text{ Kg}, L = 1.0 \text{ m}, \\ K_i &= 10.0 \text{ N-m/rad}, \Gamma_i = 1.0, G = 9.8 \text{ m/s}^2 \end{aligned}$$

and

$$B_i = 1.0 \text{ N-m-sec/rad.} \quad (5.1)$$

The desired motor position trajectory is assumed to be

$$q_d(t) = \sin(t) + \pi/2 \text{ rad.} \quad (5.2)$$

The initial position and velocity error along with the manifold terms are set to zero. The controller gains are set to

$k_L = 110, k_{\eta_i} = 5, k_{\pi_i} = 5$. It should also be noted that the controller used in the simulation assumes that the model parameters can be upper and lower bounded by $\pm 50\%$ of their nominal values. Additive bounded disturbances are also injected into the system dynamics described by (2.1), (2.2), and (2.3) of the form

$$T_L = T_{m_i} = 0.1 \sin(10t) \text{ N-m.} \quad (5.3)$$

For simulation purposes, we do not calculate the term \dot{u}_L in w_{η_i} of (3.10) and \dot{u}_{η_i} of (3.14) due to the numerical burden it places on the integration algorithm; instead we set $\dot{u}_L = \dot{u}_{\eta_i} = 0$. If the proposed controller is effective without this term, then it seems logical that the performance will only be enhanced with its inclusion.

The resulting link position tracking error, link velocity error, and actuator torques for the proposed robust tracking controller are shown in Figs. 2(a)–(d), respectively. The resulting link position tracking error, link velocity error, and actuator torques for the failure of actuator 2 at $t = 3$ s are shown in Figs. 3(a)–(d), respectively. This actuator failure is considered to be due to power loss or some other electrical problem and not a failure in which the actuator binds up and is physically unable to turn. Upon closer examination of the figures, one can see that after 3 seconds, the magnitude of actuator 1

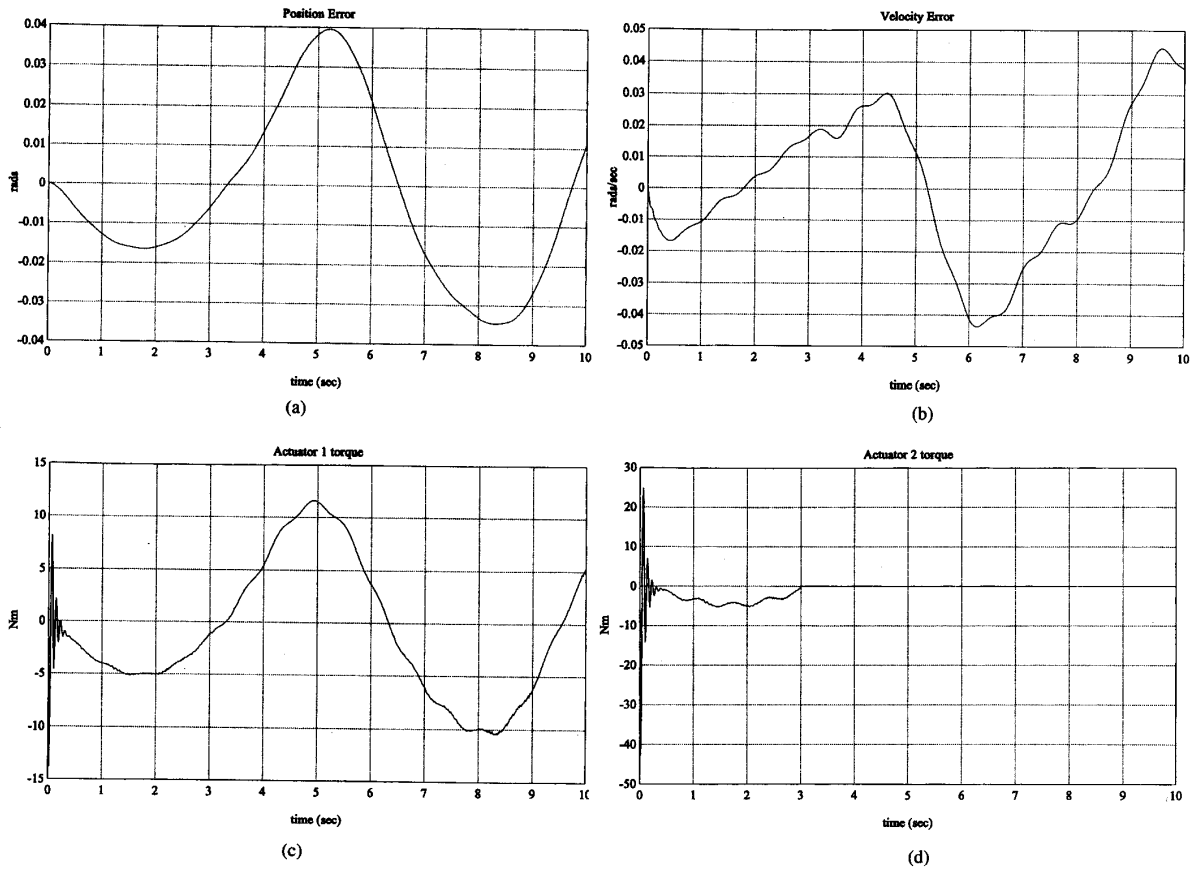


Fig. 3. Simulation results for actuator 1 operational and failure of actuator 2.

in Fig. 2(c) is smaller than that of Fig. 3(c). This indicates that actuator 1 compensates for the loss of actuator 2 with an increase in torque output. A comparison of Fig. 2(a) to Fig. 3(a) shows that the tracking error increases slightly, but good tracking is still maintained even with complete failure of one of the actuators.

VI. CONCLUSION

In this paper, we developed a robust position tracking controller for rigid-link flexible-joint (RLFJ) robots with redundant actuators. This controller achieves GUUB stability of the link tracking error in spite of additive bounded disturbances, model uncertainty, and joint flexibilities. Given a controller designed specifically for robots with redundant actuators, we can realize the benefits of such a system. Potential benefits are increased payload capacity, and prevention of total system shutdown if a joint actuator fails. We also showed in this paper how the flexibilities and gear ratios of the actuators determine how equally the load at the joints is distributed. In addition to showing GUUB stability, we illustrated how the controller gains can be adjusted to obtain better tracking performance, and gave a specific upper bound on the position tracking error transient response.

APPENDIX A

Lemma A.1

Let a dynamic state equation be described as follows:

$$\dot{x} = f(x(t), t), \quad (\text{A.1})$$

and a positive scalar function of the state $V(x(t), t)$ be upper and lower bounded by the equation

$$\lambda_1 \|z(t)\|^2 \leq V(x(t), t) \leq \gamma_2 (\|x(t)\|) \|x(t)\|^2, \quad (\text{A.2})$$

where λ_1 is a positive scalar constant, $\gamma_2(\|x(t)\|)$ is a positive scalar function, and $x(t)$ is a state vector. If the upper bound of the derivative of the scalar function with respect to time is given by

$$\dot{V}(x(t), t) \leq -\lambda_3 \gamma_2(\|x(t)\|) \|x(t)\|^2 + \epsilon, \quad (\text{A.3})$$

where λ_3 and ϵ are positive scalar constants, then

$$\|x(t)\| \leq \left[\frac{\gamma_2(\|x(0)\|)}{\lambda_1} \|x(0)\|^2 \exp(-\lambda_3 t) + \frac{\epsilon}{\lambda_1 \lambda_3} [1 - \exp(-\lambda_3 t)] \right]^{1/2}. \quad (\text{A.4})$$

$$\dot{L}_1 \leq \frac{\epsilon_L}{1 + \frac{\epsilon_L}{\rho_L \|r_L\| + G_L}} + \sum_{i=1}^2 \left[\frac{\epsilon_{\eta_i}}{1 + \frac{\epsilon_{\eta_i}}{\rho_{\eta_i} \|\eta_i\| + \epsilon_{\eta_i}}} + \frac{\epsilon_{\pi_i}}{1 + \frac{\epsilon_{\pi_i}}{\rho_{\pi_i} \|\Pi_i\| + \epsilon_{\pi_i}}} \right], \quad (\text{B.5})$$

Examination of (A.4) shows that the state vector $x(t)$ is GUUB in the sense that as time approaches infinity the norm of the state $\|x(t)\|$ is ultimately confined in a ball of size $\sqrt{\epsilon/\lambda_1 \lambda_3}$.

Proof: Using the upper bound on V in (A.2), we can rewrite (A.3) as

$$\dot{V}(x(t), t) \leq -\lambda_3 V(x(t), t) + \epsilon. \quad (\text{A.5})$$

If we multiply both sides of (A.5) by $\exp(\lambda_3 t)$, we obtain the following equation:

$$\begin{aligned} \exp(-\lambda_3 t) \dot{V}(x(t), t) + \exp(-\lambda_3 t) V(x(t), t) \\ \leq \epsilon \exp(-\lambda_3 t) \end{aligned} \quad (\text{A.6})$$

which can be rewritten as

$$\frac{d}{dt} (\exp(-\lambda_3 t) V(x(t), t)) \leq \epsilon \exp(-\lambda_3 t). \quad (\text{A.7})$$

We can use separation of variables to write (A.7) as

$$\int_0^t d(\exp(-\lambda_3 t) V(x(t), t)) \leq \int_0^t \epsilon \exp(-\lambda_3 t) dt. \quad (\text{A.8})$$

Performing the integration gives the following equation:

$$\begin{aligned} V(x(t), t) \leq V(x(0), 0) \exp(-\lambda_3 t) \\ + \frac{\epsilon}{\lambda_3} [1 - \exp(-\lambda_3 t)]. \end{aligned} \quad (\text{A.9})$$

If we use the upper and lower bound on V given in (A.2), we have the following inequalities:

$$\lambda_1 \|x(t)\|^2 \leq V(x(t), t)$$

and

$$V(x(0), 0) \leq \gamma_2 (\|x(0)\|) \|x(0)\|^2. \quad (\text{A.10})$$

Substituting (A.10) into (A.9) results in

$$\begin{aligned} \lambda_1 \|x(t)\|^2 \leq \gamma_2 (\|x(0)\|) \|x(0)\|^2 \exp(-\lambda_3 t) \\ + \frac{\epsilon}{\lambda_3} [1 - \exp(-\lambda_3 t)] \end{aligned} \quad (\text{A.11})$$

and consequently (A.11) can be written as (A.4). \square

APPENDIX B

Lemma B.1

Given a scalar function \dot{L}_1 described as by the following equation:

$$\begin{aligned} \dot{L}_1 = & \|r_L\| \|w_L\| \\ & - \sum_{i=1}^2 \left[\frac{1}{2} r_L^T \bar{K}_i k_{T_L}^{-1} v_L - \|\eta_i\| \|w_{\eta_i}\| \right. \\ & \left. + \eta_i^T v_{\eta_i} - \|\Pi_i\| \|w_{\pi_i}\| + \Pi_i^T v_{\pi_i} \right], \end{aligned} \quad (\text{B.1})$$

then

$$\dot{L}_1 \leq \epsilon, \quad (\text{B.2})$$

where ϵ is defined in (3.22).

Proof: If we substitute (3.17) into (B.1) and use the minimum bound on $\bar{K}_T = \bar{K}_1 + \bar{K}_2$ given in (2.10), we can rewrite it as

$$\begin{aligned} \dot{L}_1 \leq & \|r_L\| \|w_L\| - \frac{\lambda_{\min}\{\bar{K}_T\} \|r_L\|^2 \rho_L^2}{\bar{k}_{TL} (\rho_L \|r_L\| + \epsilon_L)} \\ & + \sum_{i=1}^2 \left[\|\eta_i\| \|w_{\eta_i}\| - \frac{\|\eta_i\|^2 \rho_{\eta_i}^2}{\|\eta_i\| \rho_{\eta_i} + \epsilon_{\eta_i}} \right. \\ & \left. + \|\Pi_i\| \|w_{\pi_i}\| - \frac{\|\Pi_i\|^2 \rho_{\pi_i}^2}{\|\Pi_i\| \rho_{\pi_i} + \epsilon_{\pi_i}} \right]. \end{aligned} \quad (\text{B.3})$$

We can substitute ρ_L , ρ_{η_i} , and ρ_{π_i} defined in (3.18) into (B.3) and use (2.9) to yield the new upper bound on \dot{L}_1 .

$$\begin{aligned} \dot{L}_1 \leq & \|r_L\| \rho_L - \frac{\|r_L\|^2 \rho_L^2}{\rho_L \|r_L\| + \epsilon_L} \\ & + \sum_{i=1}^2 \left[\|\eta_i\| \rho_{\eta_i} - \frac{\|\eta_i\|^2 \rho_{\eta_i}^2}{\|\eta_i\| \rho_{\eta_i} + \epsilon_{\eta_i}} \right. \\ & \left. + \|\Pi_i\| \rho_{\pi_i} - \frac{\|\Pi_i\|^2 \rho_{\pi_i}^2}{\|\Pi_i\| \rho_{\pi_i} + \epsilon_{\pi_i}} \right]. \end{aligned} \quad (\text{B.4})$$

(B.4) can be rewritten as (see top of page)

and by using (3.22), a final upper bound on \dot{L}_1 can be written as (B.2). \square

REFERENCES

- [1] C. Abdallah, D. M. Dawson, P. Dorato, and M. Jamshidi, "Survey of the robust control of robots," *IEEE Contr. Syst. Mag.*, vol. 11, no. 2, pp. 24–30, Feb. 1991.
- [2] R. Ortega and M. Spong, "Adaptive motion control of rigid robots: A tutorial," in *Proc. IEEE Conf. Decision and Control*, Austin, TX, 1988.
- [3] D. M. Dawson, Z. Qu, and M. M. Bridges, "Hybrid adaptive control for the tracking of rigid-link flexible-joint robots," in *Proc. 1991 ASME Winter Annu. Meeting*, vol. 31, pp. 95–97.
- [4] D. M. Dawson, Z. Qu, M. M. Bridges, and J. J. Carroll, "Robust tracking of rigid-link flexible-joint electrically-driven robots," in *Proc. 1991 IEEE Conf. Decision and Control*, vol. 2, pp. 1409–1412.
- [5] M. Readman and P. Belanger, "Analysis and control of a flexible joint robot," in *Proc. IEEE Conf. Decision and Control*, Honolulu, HI, pp. 2551–2559, 1990.
- [6] F. Mrad and S. Ahmad, "Adaptive control of flexible joint robots with stability in the sense of Lyapunov," in *Proc. IEEE Conf. Decision and Control*, Honolulu, HI, pp. 2667–1672, 1990.
- [7] F. Ghorbel and M. Spong, "Stability analysis of adaptively controlled flexible joint robots," in *Proc. IEEE Conf. Decision and Control*, Honolulu, HI, pp. 2538–2544, 1990.
- [8] J. Slotine, "Putting physics in control—The example of robotics," *Contr. Syst. Mag.*, vol. 8, pp. 12–17, Dec. 1988.
- [9] J. J. Craig, *Adaptive Control of Mechanical Manipulators*. Ann Arbor, MI: UMI Dissertation Information Service, 1986.
- [10] S. Barnett, *Matrices in Control Theory*. Malabar, FL: Krieger, 1984.

- [11] M. Spong, "Modeling and control of elastic joint robots," *J. Dynamic Syst., Measurement, Contr.*, vol. 109, pp. 310-319, Dec. 1987.
- [12] A. S. I. Zinober, Ed., *Deterministic Control of Uncertain Systems*. London, England: Peregrinus, 1990.
- [13] D. Dawson, Z. Qu, F. Lewis, and J. Dorsey, "Robust control for the tracking of robot motion," *Int. J. Contr.*, vol. 52, no. 3, pp. 581-595, 1990.
- [14] J. J. Slotine and W. Li, *Applied Nonlinear Control*. Englewood Cliffs, NJ: Prentice-Hall, 1991.
- [15] D. Dawson and Z. Qu, "Re-thinking the robust control of robot manipulators," in *Proc. IEEE Conf. Decision and Control*, vol. 1, pp. 1043-1045, Apr. 1991.
- [16] M. Vidyasagar, *Nonlinear Systems Analysis*. Englewood Cliffs, NJ: Prentice-Hall, 1978.
- [17] A. Beneallegue and N. M'Sirdi, "Passive control for robot manipulators with elastic joints," in *Proc. IMACS MCTS 91, Modeling and Control of Technological Systems*, vol. 1, Lille, France, pp. 481-487, 1991.
- [18] K. Chen and L. Fu, "Nonlinear adaptive motion control for a manipulator with flexible joints," in *Proc. IEEE Int. Conf. Robotics and Automation*, vol. 2, Scottsdale, AZ, pp. 1201-1206, 1989.
- [19] A. De Luca, "Dynamic control of robots with joint elasticity," in *Proc. IEEE Int. Conf. Robotics and Automation*, pp. 24-29, Apr. 1988.
- [20] A. Ficola, R. Marino, and S. Nicosia, "A singular perturbation approach to the control of elastic robots," in *Proc. Alerton Conf. Communication, Control, and Computing*, Univ. Illinois, 1983.
- [21] K. Khorasani and M. Spong, "Invariant manifolds and their applications to robot manipulators with flexible joints," in *Proc. IEEE Int. Conf. Robotics and Automation*, St. Louis, MO, 1985.
- [22] J. Slotine and S. Hong, "Two time scale sliding mode control of manipulators with flexible joints," in *Proc. Amer. Controls Conf.*, 1986.
- [23] P. Tomei, S. Nicosia, and A. Ficola, "An approach to the adaptive control of elastic joint robots," in *Proc. IEEE Int. Conf. Robotics and Automation*, 1986.
- [24] I. Kanallakopoulos, P. Kokotovic, and R. Marino, "An extended direct scheme for robust adaptive nonlinear control," *Automatica*, vol. 27, no. 2, pp. 247-255, 1991.
- [25] I. Kanallakopoulos, P. Kokotovic, and A. Morse, "Systematic design of adaptive controllers for feedback linearizable systems," *IEEE Trans. Automat. Contr.*, vol. 36, no. 11, pp. 1241-1253, 1991.
- [26] Z. Qu and D. M. Dawson, "Lyapunov direct design of robust tracking control for classes of cascaded nonlinear uncertain systems without matching conditions," in *Proc. Conf. Decision and Control*, vol. 3, pp. 2521-2526, 1991.
- [27] Z. Qu and D. M. Dawson, "Robust control design of a class of cascaded nonlinear systems," in *Proc. 1991 ASME Winter Meeting*, vol. 33, pp. 63-71.
- [28] R. Lozano and B. Brogliato, "Adaptive control of robot manipulators with flexible joints," *IEEE Trans. Automat. Contr.*, vol. 37, no. 2, pp. 174-181, 1992.
- [29] D. M. Dawson, "Modeling and control of the automated radiation inspection device," *Kennedy Space Center, Internal Rep.*, NASA-NGT-60002, suppl. 6, July 27, 1991.
- [30] M. W. Spong, "Control of flexible joint robots: a survey," Coordinated Science Laboratory Report UILU-ENG-90-2203 DC-116, University of Illinois at Urbana-Champaign, Feb. 1990.



Darren M. Dawson was born in Macon, GA, in 1962. He received the Associate degree in mathematics from Macon Junior College in 1982 and the B.S. (highest honors) and Ph.D. degrees in electrical engineering from the Georgia Institute of Technology in 1984 and 1990, respectively.

He worked for Westinghouse as a control engineer from 1985 to 1987, where he designed control panels for the first U.S. submarine converted into a naval training vessel. While working toward the Ph.D. degree, he also served as a research/teaching assistant and was named Outstanding Graduate Teaching Assistant during the 1988-1989 academic year. In July 1990, he joined the Department of Electrical and Computer Engineering and the Center for Advanced Manufacturing (CAM) at Clemson University where he currently holds the position of Associate Professor. Under the CAM director's supervision, he currently leads the Robotics and Manufacturing Automation Laboratory which is jointly operated by the Departments of Electrical and Mechanical Engineering. His main research interests are in the fields of nonlinear based robust, adaptive, and learning control with application to constrained mechanical systems and electromechanical systems including robot manipulators and motor drives. He has authored and coauthored over 100 journal and conference papers, 2 research monograph book chapters, and a textbook related to these subjects. In 1991, Dr. Dawson was awarded the National Science Foundation Research Initiation Award to conduct robotics research in the position/force control area.



Zhihua Qu was born in Shanghai, China, in 1963. He received the B.Sc. and M.Sc. degrees in electrical engineering from the Changsha Railway Institute in 1983 and 1986, respectively, and the Ph.D. degree in electrical engineering from the Georgia Institute of Technology in 1990.

He is now an Assistant Professor of Electrical Engineering at the University of Central Florida. His research interests are in robust control, robotics, adaptive control, power system, and nonlinear system theory.



Michael M. Bridges was born in Toledo, OH, in 1966. He received the B.S. degree in electrical engineering from the University of Michigan, Ann Arbor, in 1989 and the M.S. degree in electrical engineering from Georgia Institute of Technology, Atlanta, in 1990.

Presently he is pursuing the Ph.D. degree in electrical engineering at Clemson University, Clemson, SC. His current research interests include adaptive and robust control of flexible joint robots, flexible structures, and the analysis of mechanical systems with harmonic drive gearing and belt-driven transmission devices.



Scott C. Martindale was born in Philadelphia, PA, on May 31, 1963. He received the B.S. degree in physics from Bob Jones University in 1990 and the M.S. degree in electrical engineering from Clemson University in 1992.

He is currently working on the Ph.D. degree in electrical engineering at Clemson University. His current research interests include robust control, control of flexible joint robots, and model reference control.